JOURNAL OF CATALYSIS **163,** 354–364 (1996)
ARTICLE NO. 0337

The Nature of Vanadium in Vanado-Silicate (MFI) Molecular Sieves: Influence of Synthesis Methods

T. Sen, P. R. Rajamohanan, S. Ganapathy, and S. Sivasanker

National Chemical Laboratory, Pune 411008, India

Received January 11, 1996; revised June 3, 1996; accepted July 15, 1996

The influence of synthesis in acidic or alkaline media on the incorporation of vanadium in the MFI (ZSM-5) lattice has been studied. An alkaline gel favors the incorporation of vanadium in the MFI framework, while an acidic gel does not. EPR and analytical data indicate that mostly V^{4+} species are present in an octahedral (Oh) environment in the as-synthesized V-MFI prepared in acidic media, which latter transform into polymeric V^{5+} species on calcination. In the alkaline media, vanadium is incorporated mostly as V^{5+} in a distorted Td environment. Thermal analysis and XRD data indicate that phase transformation from orthorhombic to monoclinic takes place during the calcination process only when the sample is prepared from acidic medium. It is found that the sample prepared from alkaline medium contains Si–OH groups from defect centers while such groups are absent in the sample prepared in acidic medium. It appears that V-ions are present in the defect sites in the MFI framework in the sample prepared from alkaline medium.

INTRODUCTION

Studies on the incorporation of transition metal ions, particularly titanium and vanadium, in zeolite lattices are important as these transition metal analogs are catalytically active in various shape selective oxidation reactions useful in the synthesis of fine chemicals. Though earlier workers (1–10) have suggested that vanadium is incorporated in the framework as V^{4+}, recent studies have revealed that vanadium incorporation takes place as V^{5+} in the lattice of KVS-5 (11), BEA (12), and MEL (13) molecular sieves. It is also expected that the incorporation of smaller V^{5+} ($r = 0.046$ nm) should be more favorable than V^{4+} ($r = 0.059$ nm) in the Si^{4+} ($r = 0.026$ nm) lattice. The lattice V^{5+} species are easily reducible to V^{4+} species. Whittington *et al.* (14) have reported that the reduction takes place due to the reactivity (reducibility) of the V–O–Si bonds rather than V=O. All the above reports (11–13) deal with the incorporation of vanadium in alkaline media but so far, no reports are available in the literature about vanadium incorporation in acidic media. A low pH synthesis of zeolite by the "fluoride method" has been reported recently (15–17). This method leads to the production of large defect free crystals. Centi *et al.* (18) and Moudrakovski *et al.* (19) have reported that the location of lattice vanadium species is near the defect sites and the incorporation is related to the amount of defect sites. Our present studies deal with the identification of different V-species present in acidic and alkaline gels and the crystalline phases prepared from them. The influence of the mode of preparation on the incorporation of vanadium in the lattice of silicalite-1 and the catalytic activities of the samples are being reported.

EXPERIMENTAL

Two vanado-silicate (MFI) samples A and B were synthesized from acidic and alkaline media, respectively. The synthesis (sample A) in the acidic medium was carried out as follows: NH_4F (2.47 g) and tetrapropyl ammonium bromide (TPABr; 4.44 g) were dissolved in water (40 g) and mixed with an aqueous solution of $VOSO_4$ (0.18 g in 44 g water). The resultant solution was blue in color. Fumed silica (Sigma, 4 g) was added slowly to the above solution over a period of 1 h with vigorous stirring. After complete addition of the fumed silica, the resultant gel was gray in color. This was stirred for another hour. The pH of the gel was 6.8. The molar composition of the final gel was $SiO_2 : 0.0125\ VO_2 : 0.25\ TPABr : NH_4F : 70\ H_2O$. The gel was allowed to crystallize at 473 K for 7 days under static conditions in a teflon-lined autoclave. The grayish white material (sample A) was dried at 373 K and calcined at 823 K for 12 h. The calcined material was white under dehydrated conditions. On hydration it became deep yellow.

The synthesis of the V-MFI sample in alkaline medium (sample B) was carried out as per published procedures (1–4, 18). The molar composition of the synthesis gel was $SiO_2 : 0.0125\ VO_2 : 0.33\ TPAOH : 22\ H_2O$ (TPAOH = tetrapropyl ammonium hydroxide (Aldrich)). $VOSO_4$, $3H_2O$ was used as the vanadium source and tetraethyl orthosilicate was used as the silica source. The pH of the light green gel was 11.1. The crystallization was carried out in a sealed autoclave under static conditions at 443 K for 2 days. The crystalline material was filtered, washed, dried (383 K), and calcined (823 K for 12 h). The calcined material was pale yellow in hydrated and dehydrated conditions.

0021-9517/96 $18.00

TABLE 1

V^{4+} and V^{5+} Break-Up in the Gel and Crystalline Samples

		V-content ($\times 10^{-3}$)								
					Crystalline material					
		Gel			As-synthesized			Calcined		Extracted
Sample	pH of gel	V/Si + V	V^{4+}/Si + V	V^{5+}/Si + V	V/Si + V	V^{4+}/Si + V	V^{5+}/Si + V	V^{4+}/Si + V	V^{5+}/Si + V	V/Si + V
A	6.8	12.5	12.2 (11.8)[a] (11.4)[b]	0.3	10.2	10.2 (9.5)	—	0.5 —	9.7	1.1
B	11.1	12.5	4.1 (11.9)[a] (3.9)[b]	8.4	5.4	1.2 (0.9)	4.2	— (3.7)[c]	5.4	3.9 (3.4)[c]

Note. Values within brackets have been estimated from EPR.
[a] Initial concentration of V^{4+} in gel (see text).
[b] Final concentration of V^{4+} in gel (see text).
[c] Concentration of V^{4+} in reduced samples.

The calcined samples (A and B) were next treated with 1 *N* NH_4OAc solution at 353 K for 12 h to remove the extralattice vanadium (18). Extraction with NH_4OAc at room temperature has been found by earlier authors to remove the extralattice vanadium (18). After the NH_4OAc treatment, samples A and B were calcined at 723 K (6 h) in air and the resultant materials were white even after hydration.

Analysis of the gel and the crystalline phases were carried out for both V^{4+} and V^{5+} ions by established titrimetric methods (20) using a standard $KMnO_4$ solution (for the estimation of V^{4+}) and standard Mohr's salt solution with sodium diphenylamine sulfonate as an indicator (for the estimation of V^{5+}; Table 1). XRD patterns of the samples were obtained using Cu$K\alpha$ radiation (Rigaku, Model DMAX-III VC). EPR spectra of the liquids and the solids were recorded in a Bruker ER 200D model spectrometer at 9.73 GHz (*X* band) using a standard sample (weak pitch; Varian, $g = 2.0029$). The estimation of V^{4+} in the gel as well as in the solid phases was performed by integrating the EPR spectra and comparing with a series of V-impregnated silicalite-2 samples (standards) containing known quantities of V^{4+} and V^{5+} ions. A broad background was observed in the spectra of both the standards and unknown samples; no corrections for the background were made. The total area of the spectrum was calculated by adding the areas of the hyperfine peaks; a plot of the areas of the standards was made against the concentration of the paramagnetic V^{4+} species. The V^{4+} concentration in the unknown material was estimated using this calibration plot. Diffuse reflectance spectra were recorded using a UV–visible spectrometer (model UV-2101 PC, Shimadzu). The framework infrared spectra were recorded with a PC-based FTIR (Perkin Elmer; PC16) spectrometer using KBr pellets. The liquid and solid state ^{51}V NMR, ^{29}Si MAS, ^{1}H MAS, and ^{13}C CP-MAS NMR spectra were recorded in a Bruker MSL 300 spectrometer. $VOCl_3$ and tetramethyl silane were used as the standards.

The oxidation of toluene using H_2O_2 (28% aqueous solution) as the oxidant was performed in a batch reactor at 353 K. The products were analyzed by gas chromatography (Model HP 5880; capillary column, 50 m × 0.5 mm, cross-linked methyl silicone gum).

RESULTS AND DISCUSSION

Analytical Data

Both the samples A and B were prepared using $VOSO_4$, $3H_2O$ possessing V in the V^{4+} state. However, when the precursor gels are analyzed the acidic gel is found to contain mostly V^{4+} while the alkaline gel contains more V^{5+} than V^{4+} ions (Table 1). The aerial oxidation of V^{4+} to V^{5+} is known to occur rapidly in alkaline media (21). The as-synthesized crystalline sample A contains mostly the V^{4+}, whereas sample B contains mostly V^{5+} (Table 1). When the as-synthesized samples are calcined, only V^{5+} species are present in sample B, whereas, sample A retains a small amount of V^{4+}. On extraction with 1 *N* NH_4OAc solution, most of the vanadium (89%) is extracted out from sample A, while a much smaller amount of vanadium (28%) is extracted out from sample B.

X-Ray Diffraction

The as-synthesized forms of both the samples were highly crystalline with an orthorhombic structure (Figs. 1a and 1b). Upon calcination, sample A changes its symmetry to monoclinic (revealed by the splitting of the line at $2\theta = 24.38^\circ$ (22)), while sample B retains the orthorhombic symmetry (Fig. 1; compare a, a′ and b, b′). Earlier workers (23) have reported that silicalite-1 and TS-1 containing less than

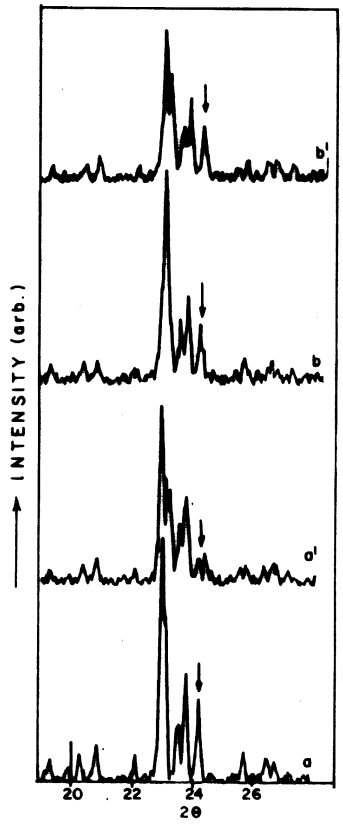

FIG. 1. XRD patterns of the samples. Sample A: as-synthesized (a) and calcined (a′); sample B: as-synthesized (b) and calcined (b′).

1Ti/UC change symmetry on calcination, while TS-1 containing more Ti did not. In the case of our sample B, no change in symmetry is observed even though it contains only about 0.5 V/UC. While a change in symmetry need not be an evidence for nonincorporation (as in sample A), the absence of a symmetry change in B does suggest that V-ions are probably present in the framework positions in sample B. However, the presence of extraneous matter in the zeolite pores, such as adsorbates (24) and the presence of faults (defects) (25) could prevent such a symmetry change. When silicalite-1 was loaded (by impregnation) with 1 wt% V and calcined, the symmetry change took place. The above observation and the observation of a symmetry change in sample A (containing nearly double the amount of V as sample B) suggest that the reason for the absence of symmetry change of B is probably due to the presence of V in the framework (and not due to the V being present as occluded oxides). However, the simultaneous creation of defect sites along with V-incorporation could also explain the absence of the symmetry change. Moreover, a slight shift in the position of the 100% peak ($2\theta = 23.2^\circ$) for the calcined sample B is noticed, when compared to pure silicalite-1 indicating a small increase in the unit cell size of B. No such difference is observed for the sample A. As V-ions are much larger than Si^{4+} ions, an increase in the unit cell size is expected if V-ions are present in the framework. In fact, earlier studies (13) have shown that the expansion of the unit cell volume is related to the concentration of the framework (nonextractable) vanadium in the samples. The XRD studies and the NH_4OAc extraction results suggest that while a little or no V-ions are present in the framework of sample A, sample B contains significant quantities of framework V-species.

Scanning Electron Microscopy (SEM)

The SEM picture of sample A (Fig. 2a) reveals mostly large (6–8 μm) twinned hexagonal crystallites. Sample B (Fig. 2b) consists of spheroidal crystallites of 0.1–0.2 μm.

EPR Spectroscopy

The EPR spectra of the precursor gels of samples A and B exhibit eight line hyperfine spectrum without anisotropy ($g = 1.963$ and $A = 92.8$ G) (Figs. 3a and 3b) immediately

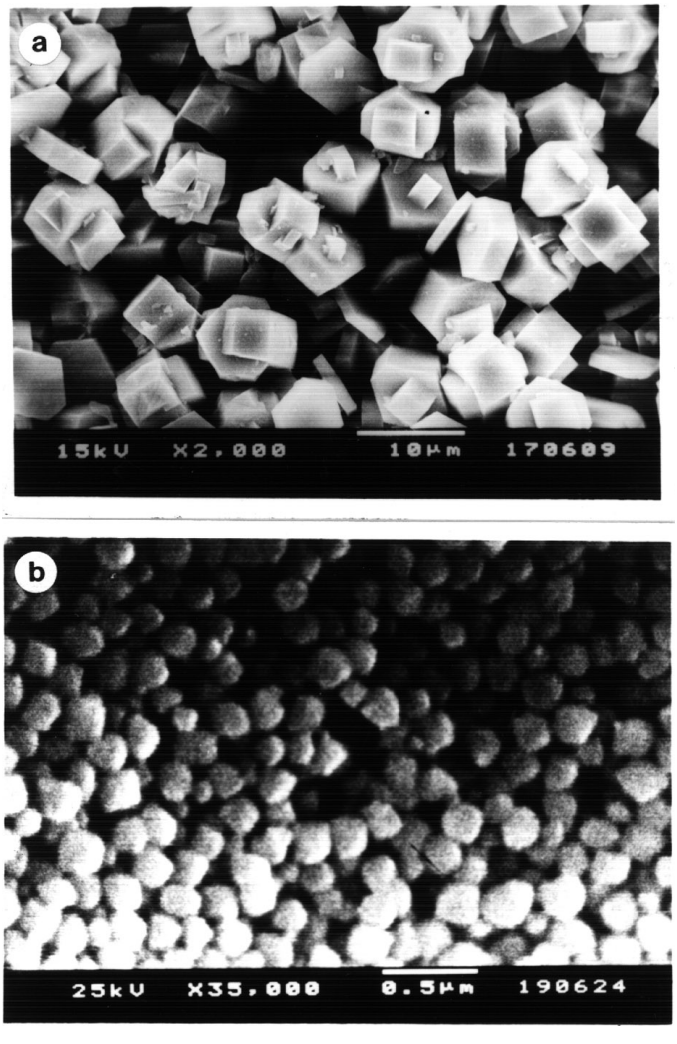

FIG. 2. SEM photographs of the samples. Sample A (a) and sample B (b).

after preparation (0 h). On ageing the acidic gel at 298 K for 2 h, the spectrum is similar to the fresh one (Fig. 3a), while the spectrum of gel B after ageing for 4 h reveals an eight-line hyperfine spectrum (Fig. 3b) with anisotropy ($g_\parallel = 1.923$, $g_\perp = 1.981$, $A_\parallel = 185.2$ G, $A_\perp = 79.8$ G). The EPR spectra suggest that free VO^{2+} ions are present in the fresh and aged gels of A (Figs. 3a and 3a′; Table 1) and that while free VO^{2+} ions are present in the fresh gel of B, they are present in an axially symmetric environment in the aged gel of B (Figs. 3b and 3b′; Table 1). The intensity of the spectrum of the final alkaline gel is less than that of the final acidic gel (Figs. 3a and 3b; Table 1), although the same amount of V^{4+} was added during the preparation of the gel, due to transformation of the V^{4+} ions into V^{5+} ions in the alkaline medium.

The as-synthesized sample A exhibits a eight-line hyperfine spectrum (Fig. 4a) with a broad background. The EPR parameters ($g_\parallel = 1.935$, $g_\perp = 1.982$, $A_\parallel = 188.5$ G, $A_\perp = 82$ G) indicate that the V species are in a distorted Oh environment. It is possible that the broad band is associated with agglomerated V^{4+} ions. However, this does not appear

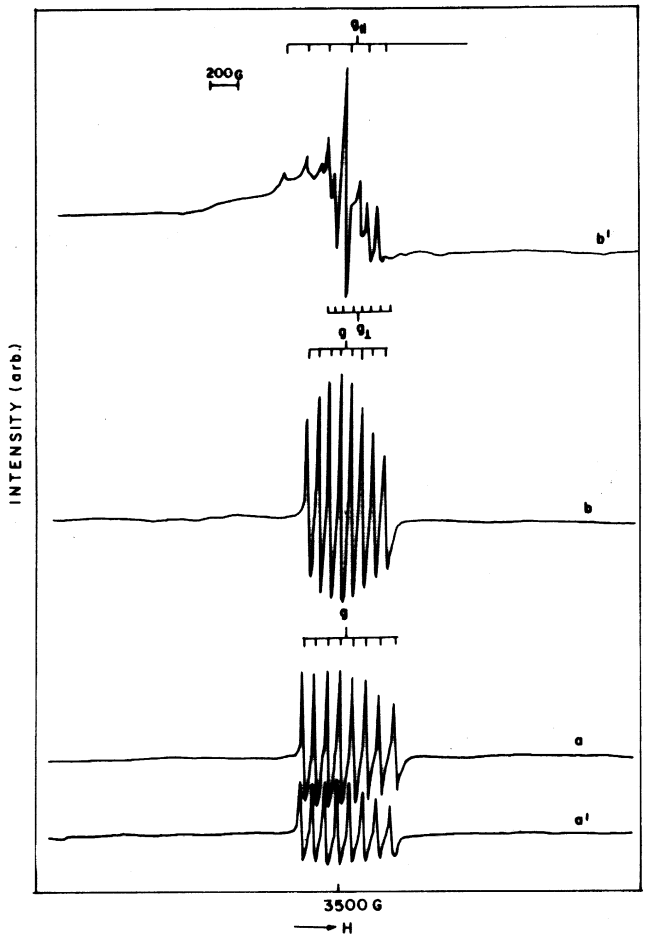

FIG. 3. EPR spectra of the synthesis gels. Gel A: initial, 0 h (a), and final, 2 h (a′); gel B: initial, 0 h (b), and final, 4 h (b′).

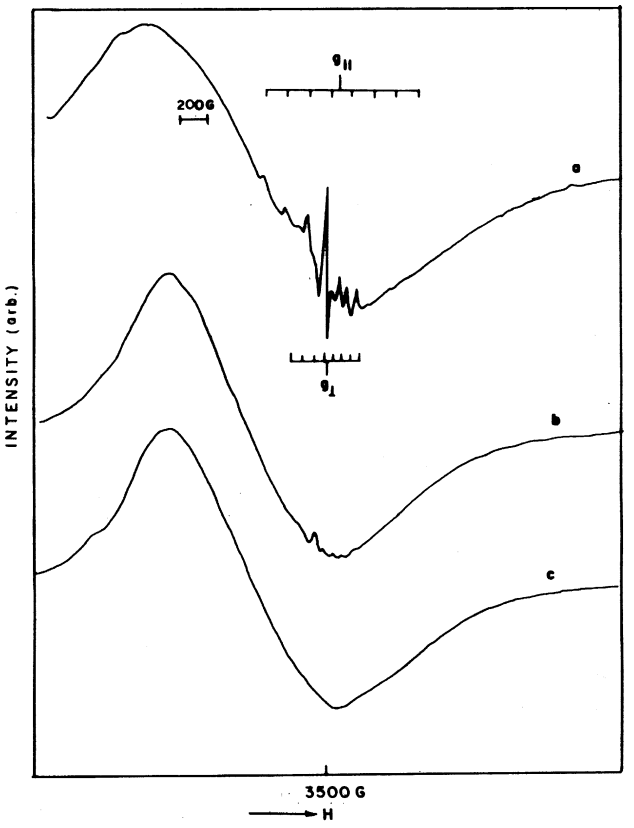

FIG. 4. EPR spectra of the V-MFI synthesized in acidic medium (sample A): as-synthesized (a), calcined (b), and reduced (c).

likely as even the calcined sample (in which all the V^{4+} ions are expected to be transformed into V^{5+}) exhibits that band with about the same intensity (Fig. 4b). More investigation into the origin of the broad band is necessary. The intensity of the sharp hyperfine lines attributed to better dispersed V^{4+} becomes very small on calcination suggesting the near total oxidation of the V^{4+} ions into V^{5+}. Upon reduction in H_2 at 573 K (6 h), the V^{4+} hyperfine lines do not reappear (Fig. 4c), suggesting that the V^{4+} species which exhibited the lines in the as-synthesized sample (A) has become irreversibly oxidized.

The results of the quantitative analysis of the EPR spectra of the crystalline samples reveal that the V^{4+} contents of the samples estimated by EPR and chemical methods are of similar magnitude. The sample B exhibits an eight line EPR signal (Fig. 5a), with a weak broad background. The EPR parameters ($g_\parallel = 1.932$, $g_\perp = 1.982$, $A_\parallel = 185.1$ G, $A_\perp = 73.2$ G) indicate that V^{4+} is present in a distorted Oh environment (26, 27). Upon calcination, no EPR signal attributable to V^{4+} ions is observed (Fig. 5b) due to the complete conversion of V^{4+} to V^{5+}. On reduction in H_2 (at 573 K for 6 h), an intense eight line hyperfine spectrum (Fig. 5c) is obtained, indicating that the vanadium in sample B is easily reduced. The EPR parameters of the reduced sample of B ($g_\parallel = 1.931$, $g_\perp = 1.991$, $A_\parallel = 180.5$ G,

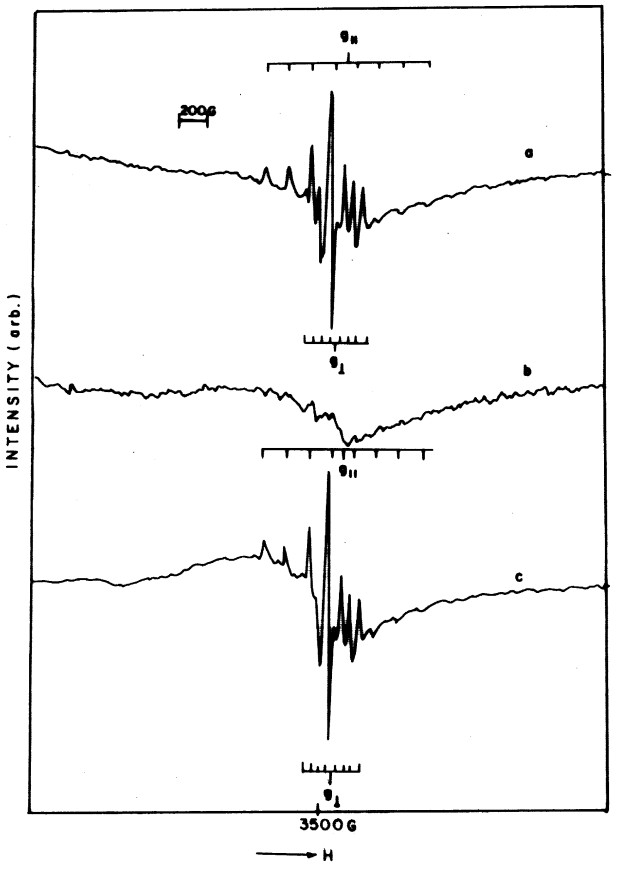

FIG. 5. EPR spectra of the V-MFI synthesized in alkaline medium (sample B): as-synthesized (a), calcined (b), and reduced (c).

$A_{\perp} = 69.5$ G) correspond to V^{4+} in a squarepyramidal environment (28). The reduced forms of both the calcined and extracted forms of sample B contain about the same amount of V^{4+} ions (Table 1) as the V^{5+} ions present before reduction, showing the easy reducibility of these ions.

UV–Visible Diffuse Reflectance (DR) Spectra

Assignments for absorptions in the UV–Vis range by solid vanadium compounds and V-silicates are shown in Table 2. Recently, Kornatowski *et al.* (11) have reported the presence of 340- and 295-nm DR bands in the as-

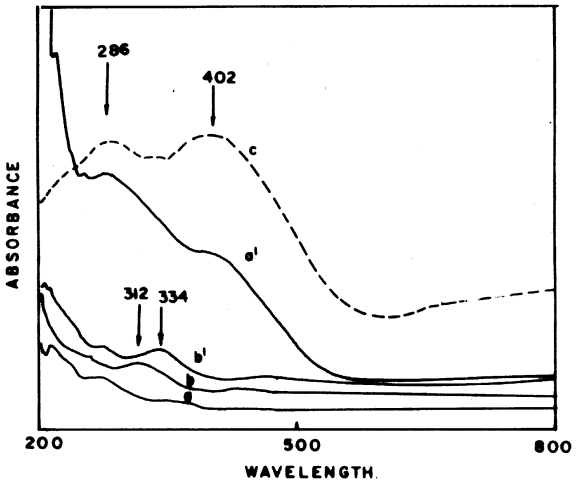

FIG. 6. UV–visible DR spectra of the different samples. Sample A: as-synthesized (a) and calcined (a′); sample B: as-synthesized (b) and calcined (b′); V-impregnated Cab-o-sil (c).

synthesized forms of the V-silicalite, KVS-5 and have attributed them to Td–V^{5+} species. The UV–visible DR spectra (Figs. 6a and 6b) of the as-synthesized forms of both the samples can be analyzed based on the above assignment. The as-synthesized form of sample A does not exhibit any band in the region 250–340 nm (Fig. 6a), suggesting the absence of detectable amounts of V^{5+} in Td environments (33, 34), but sample B exhibits a band at 312 nm (Fig. 6b), indicating the presence of V^{5+} in Td environments. The calcined form of the sample A exhibits an intense band at 286 and 402 nm (Fig. 6a′) corresponding to Td– and Oh–V^{5+} species. Cab-o-sil impregnated with NH_4VO_3 exhibits intense DR bands (Fig. 6c) at 286 and 402 nm. The positions of those bands are similar to those of the calcined sample A. This indicates that the V-species present in sample A (after calcination) are similar to the impregnated samples. The calcined form of the sample B exhibits a band at 334 nm (Fig. 6b′), corresponding to Td–V^{5+} species.

FTIR Spectroscopy

The framework ir spectra of the titanium silicalites TS-1 (35), and TS-2 (36), and vanadium containing zeolites

TABLE 2

Assignment of UV–Vis Absorption Bands by V-Ions

Metal oxidation state	Transition energy (nm)	Type of transition	Ionic environment	References
V^{5+} (pure compounds)	333–500	Charge transfer O → V	Oh	(29–32)
V^{5+} (pure compounds)	285–333	Charge transfer O → V	Td	(33, 34)
V^{4+} (pure compounds)	769	d–d	—	(18)
V^{4+} (VO^{2+})	250–285	Charge transfer O → V	—	(18)
V-MFI	384	Charge transfer O → V	Td	(18)
V-MEL	333	Charge transfer O → V	Td	(13)
KVS-5	340	—	Td	(11)

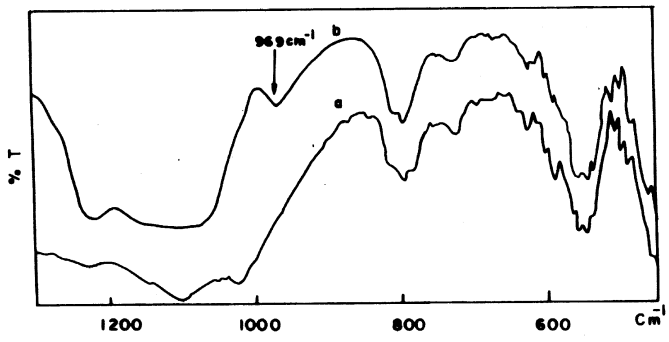

FIG. 7. Framework IR spectra of the calcined samples. Sample A (a) and sample B (b).

V-ZSM-48 (9), V-Al-Beta (12), and VS-2 (5) have already been reported. In all the cases, an IR band at around 967 cm^{-1}, not present in the Ti (or V) free analog, is noticed. The band has been attributed to $Si–O^-$ vibrations (37) and is believed to be a proof for the presence of the metal (*M*) ions in the framework (38). The spectra of the calcined samples A and B are shown in Fig. 7. The 969-cm^{-1} band is observed only in the spectrum of sample B.

Thermal Analysis

The TG and DTA curves of the as-synthesized samples A and B are shown in Fig. 8. A single exotherm is observed for the combustion of the template in the temperature range 723–823 K for sample A, while a more complex (multiple) exotherm is observed for sample B. Besides, the onset of the exotherm and the occurrence of the peak maximum (of the major exotherm) are earlier in sample B. These differences suggest that the template interacts significantly with V-ions in sample B and not in sample A. The interaction between the template and V-ions in sample B suggests that the V-ions are present in the framework in this sample. Another interesting difference is the presence of a broad and weak exotherm (without weight loss) in the temperature range 513–557 K in the DTA curve of sample A, and which is not readily apparent in that of sample B. It is likely that this exotherm is due to the phase transformation of the sample (A) from orthorhombic to monoclinic (see XRD Section). Earlier workers (22) have reported (based on XRD studies) that the symmetry change (orthorhombic to monoclinic) occurs in the temperature range 513–557 K for MFI zeolites.

NMR Spectroscopy

The liquid-state ^{51}V NMR spectrum of the gels A and B are shown in Fig. 9. The gel of sample A does not exhibit any NMR signal indicating the absence of detectable amounts of V^{5+} ions (Fig. 9a). The gel of sample B produces an intense signal at $\delta = -533$ ppm along with weak signals at $\delta = -558$ and -565 ppm (Fig. 9b). The signal at $\delta = -533$ ppm corresponds to HVO_4^{2-} species (39, 40). This

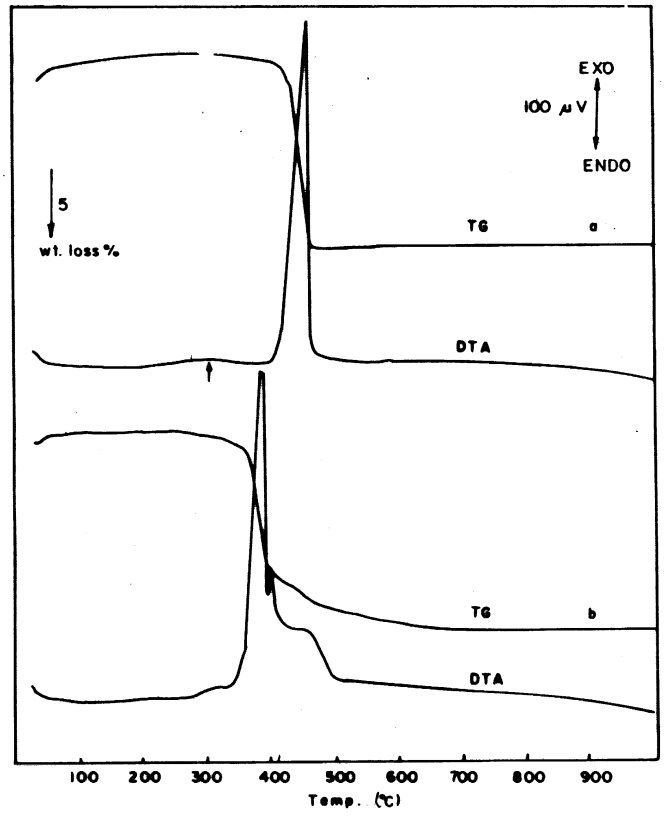

FIG. 8. TG-DTA curve of the as-synthesized samples. Sample A (a) and sample B (b).

is the major V^{5+} species suggested to be present at pH > 10 (21). The signals at $\delta = -558$ and -565 ppm are probably due to $V_2O_7^{4-}$ and its protonated form, $HV_2O_7^{3-}$, respectively. The exact assignment of the signals, however, is difficult as the chemical shift of many V-species are close to each other and the values are dependent on the pH of the solution.

Solid state NMR spectra of ^{51}V ($I = 7/2$) has recently been reviewed by Lapina *et al.* (41). ^{51}V possesses a nuclear

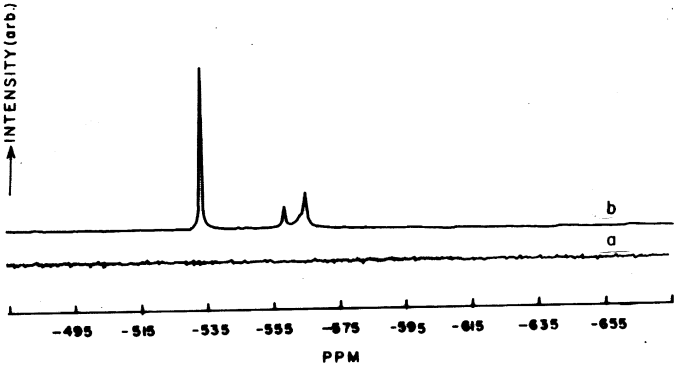

FIG. 9. Liquid state ^{51}V NMR spectra of the synthesis gels after aging. Gel A (a) and gel B (b).

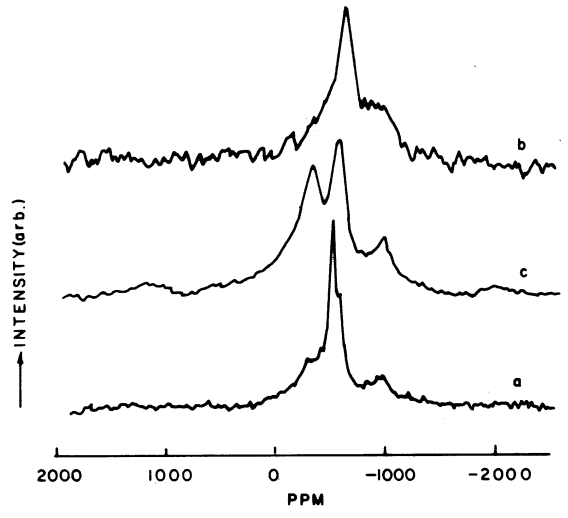

FIG. 10. ^{51}V static NMR spectra of the calcined samples. Sample A (a), sample B (b), and V-impregnated Cab-o-sil (c).

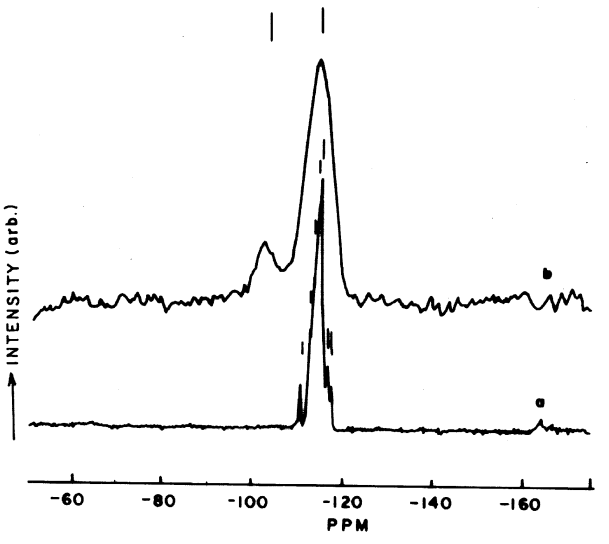

FIG. 11. ^{29}Si MAS NMR spectra of the calcined form of the samples. Sample A (a) and sample B (b).

quadrupole moment along with chemical shift anisotropy due to an asymmetric electric environment. The line shape of the ^{51}V static NMR spectrum and the isotropic chemical shift (from ^{51}V MAS NMR) could give useful information about the local environment of vanadium. ^{51}V static NMR spectra and NMR parameters have been reported by many authors (42, 43). The solid state ^{51}V static NMR of calcined samples A and B are shown in Fig. 10. Sample A exhibited a strong signal (Fig. 10a) at −502 ppm (δ_2) along with weaker signals at −284 ppm (δ_1) and −975 ppm (δ_3). Earlier workers (41) have attributed the signals at −284 and −975 ppm to octahedral V-species similar to V_2O_5, and the signal at −502 ppm to vanadium in a Td environment as in polymeric NH_4VO_3. The static ^{51}V NMR spectrum of a sample of Cab-o-sil impregnated with NH_4VO_3 is presented in Fig. 10c. The spectrum is distinctly different from those of both A and B suggesting that a major amount of the V-species present in sample A and B are different from those in the impregnated sample. After NH_4OAc treatment, the calcined sample A does not show any NMR signal due to the extraction of most of the vanadium (see Table 1). Sample B gives a nearly anisotropic spectrum (Fig. 10b) with a peak maximum at −555 ppm. A nearly identical static spectrum has been reported for the framework V-species in VS-12 (19). The spectrum has been attributed to a distorted Td environment. Based on ^{51}V MAS NMR studies of the V-MEL system, we have already reported the plausible structures for the V-species in V-MEL (13) (see Scheme 1).

It is likely that the structure of the V-species in VS-1 (MFI) are also similar to those shown above.

^{29}Si MAS NMR spectrum of the calcined sample A shows seven lines (Fig. 11a) in the chemical shift range from $\delta = -111$ to −118 ppm, corresponding to Q^4–Si sites (44). The absence of signals in the range $\delta = -98$ to −102 ppm indicate the absence of defect sites (SiOH) (16). Besides, Axon *et al.* (17) reported a broad spectrum for Fe–silicalite-1 prepared in fluoride medium, the broadness being attributed to the iron–silicon connectivity in the framework. The sharp, resolved spectrum of sample A (Fig. 11) indicates that the vanadium present in it does not have any effect on the silicon environment, presumably due to lack of V−O−Si linkages in the framework. The ^{29}Si MAS NMR spectrum of the calcined sample B shows two broad lines (Fig. 11b). The signal at −102 and −114 ppm correspond to the defect silanol and Q^4–Si sites. The broadness of the lines in this spectrum is interesting. According to Moudrakovski *et al.* (19) the broadening of the lines in the spectrum can be an indirect indication of the statistical distribution of the vanadium in the lattice.

^1H MAS NMR spectra of the calcined sample A and B are presented in Fig. 12. The signal at $\delta = 4.8$ ppm corresponds to adsorbed water. This has been confirmed by the

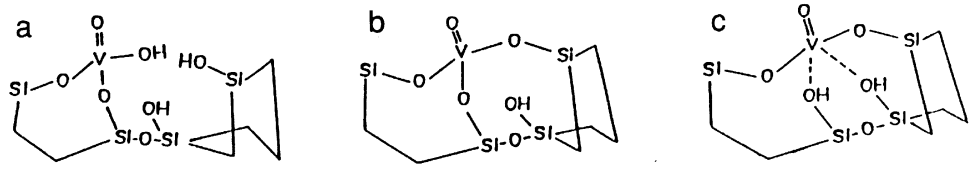

SCHEME 1. Plausible structures for the V-species in V-MEL: as-synthesized (a), calcined (b), and reduced (c).

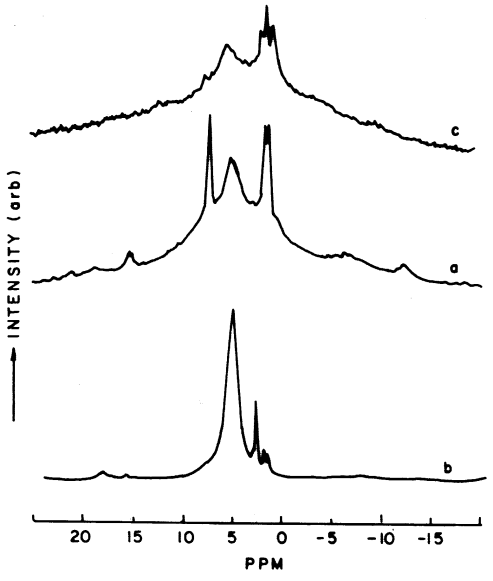

FIG. 12. ^{1}H MAS NMR spectra of the calcined form of the samples. Sample A (a), sample B (b), and NH_4OAc extracted sample A (c).

enhancement of signal intensity on stepwise hydration. The peak at 2.5 ppm of sample B (Fig. 12b) is in the chemical shift range of Si–OH (44). The signal position at 7.1 ppm (sample A) may be attributed to V–OH based on a similar assignment for Ti–OH (45). The absence of this signal in sample B also tallies with the structure of the V-species proposed by us for the calcined sample; no V–OH linkages are present. The signals at 1.6 and 1.2 ppm are probably due to two distinct ^{1}H environment and are present in both the samples, the intensities being more in sample A. The two peaks cannot be assigned to silanol groups as these would have been reflected on the ^{29}Si MAS NMR spectrum of sample A (signals would have appeared in the $\delta = -98$ to -102 ppm range). It is therefore possible that these are associated with the extralattice V-ions which are mostly present in sample A. More evidence for these peaks being due to V–OH groups is obtained from ^{1}H NMR spectrum of sample A after extraction with NH_4OAc (Fig. 12c). All the signals attributed to V–OH have decreased significantly. Besides, the ^{1}H NMR spectrum of silicalite-1 did not reveal these bands. However, interestingly, the bands were also not seen in V-impregnated silicalite-1. The slightly broader spectrum of sample A compared to sample B is due to the presence of small amounts of paramagnetic V^{4+} ions in the former (see section on EPR).

^{13}C-CP MAS NMR spectrum of the as-synthesized sample of A and B are shown in Fig. 13. Such spectra have already been reported for the as-synthesized silicalite-1 prepared in fluoride and alkaline medium (16). The similar type of splitting for C_α, C_β, and C_γ-indicate that the orientation of template in silicalite-1 is nearly the same as in vanadium-containing silicalite-1.

Catalytic Activities

The catalytic activities of samples A and B (after various treatments) in the oxidation of toluene with H_2O_2 are presented in Table 3. The reaction rates over the different samples have been reported as Turn Over Number (TON = No. of moles of toluene converted during the reaction period/mol of V present in the amount of catalyst used). Both the samples A and B lost V to different extents after the first reaction cycle due to dissolution of vanadium in the reaction medium due to the formation of soluble peroxy vanadium complexes. However, after the second cycle, negligible V-loss was detected from both samples A and B. After the first cycle, the V lost by sample A was 92%, while it was about 23% for sample B. Similar loss by the two samples was also established by NH_4OAc treatment (Table 1). The TON over sample A was 14 in the first cycle and 2 in the second cycle based on V-content in the fresh calcined sample. However, if the TON were calculated based on the V actually present in the sample after NH_4OAc extraction or after the first cycle, the values are 17 and 22. On the other hand, the TON values of the fresh sample B and after one cycle (respectively) are 120 and 111 based on the original V-content and 153 and 162 based on the actual V-content after one cycle and after extraction with NH_4OAc. The V-impregnated sample (C) and NH_4VO_3 (D) also behaved similar to sample A (Table 3). In the case of sample A, maximum conversion was reached within 2 h, whereas, in the case of sample B, the conversion increased upto about 12 h, further conversion not being possible due to depletion of H_2O_2 due to decomposition (Fig. 14). It appears that the vanadium species in sample A are rapidly extracted into

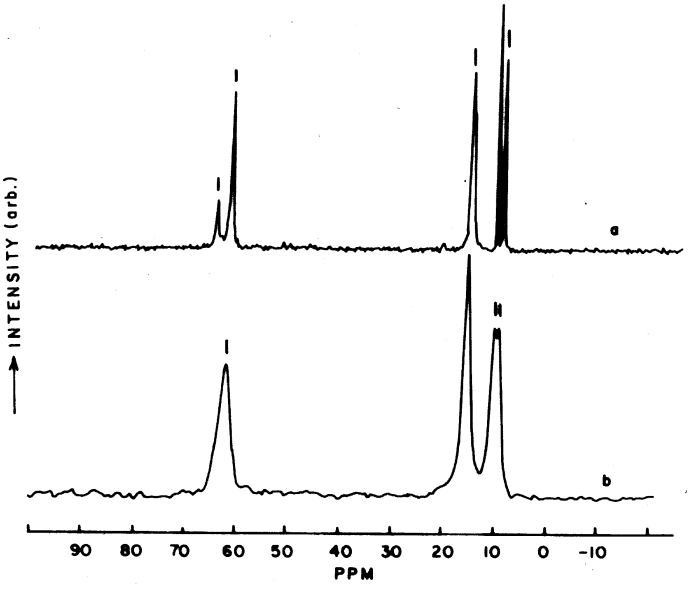

FIG. 13. ^{13}C CP-MAS NMR spectra of the as-synthesized form of the samples. Sample A (a) and sample B (b).

TABLE 3

Oxidation of Toluene over V-MFI Samples

Sample	Turnover no. (TON)[a]	H_2O_2 selectivity[b]	Product distribution (mol%)				
			Benzaldehyde	Benzyl alcohol	*o*-Cresol	*p*-Cresol	*o*/*p*[c]
A	14	11.6	52.8	8.2	21.4	17.6	1.21
B	120	52.1	41.5	11.9	23.0	23.6	0.97
A[d]	22 (2)[e]	2.6	87.8	12.2	—	—	—
B[d]	153 (111)[e]	47.5	40.8	10.9	23.2	25.1	0.92
A[f]	17	1.9	88.2	11.8	—	—	—
B[f]	162	50.3	41.2	11.4	23.5	23.9	0.98
C[g]	12	11.8	74.3	6.3	10.9	8.4	1.24
D[h]	12	13.7	68.9	4.2	14.4	12.5	1.15

Note. Reaction conditions: Cat: 0.1 g; toluene/H_2O_2 (mole) = 2; temp. = 353 K; toluene/cat (wt) = 10; solvent (acetonitrile) = 10 ml.

[a] Number of moles of toluene converted in 12h/moles of V in catalyst sample used.

[b] %H_2O_2 selectivity = Number of moles of H_2O_2 utilized in product formation/total number of moles of H_2O_2 added during the reaction.

[c] Ratio of *o*-cresol to *p*-cresol in the product.

[d] Used catalyst (second cycle).

[e] TON calculated based on vanadium present in fresh sample.

[f] NH_4OAC extracted samples.

[g] C = V-impregnated Cab-o-sil (V/Si + V = 1×10^{-2}).

[h] D = pure NH_4VO_3 (V equivalent to that in 0.1g of C).

solution by H_2O_2 (V-peroxo complexes) leading to maximum toluene conversion within 2 h, while in the case of B, the reaction proceeds slowly due to presence of the framework V-ions inside the pores of the sample and consequent diffusion limitations. The extracted V-ions (from sample A) apparently are much less active than the V-ions present in the molecular sieve. This is further confirmed by the poor activity of NH_4VO_3. The mechanism for the oxidation of hydrocarbons over VS-2, suggested by Ramaswamy *et al.* (6) implies that V-ions with redox characteristics are catalytically active, and we have already noted (EPR section) that the V^{5+} -ions in sample B undergo reduction easily.

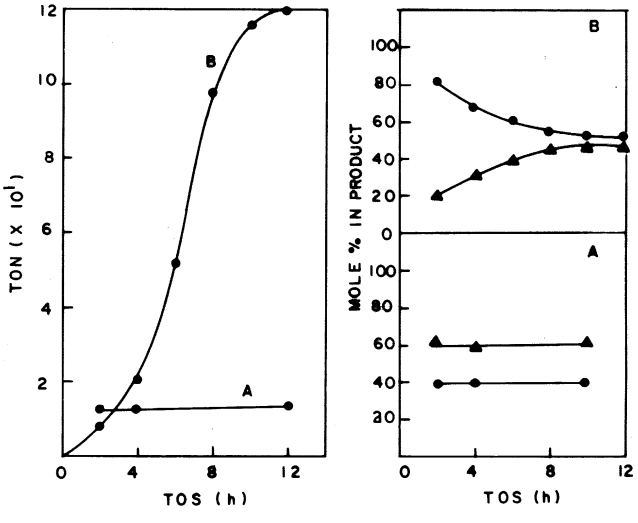

FIG. 14. Toluene oxidation over V-MFI: Influence of duration of run on conversion and product distribution. (A) Sample A, (B) sample B, (●) side chain oxidation products, and (▲) cresols.

Interestingly, the shift in the product pattern with duration of run is different for the two catalysts (Fig. 14). In the case of B, the yield of the side chain oxidation products decreases and the yield of the cresols increases with time, whereas, in the case of A, the relative yield of the two types of products remains nearly constant (Fig. 14). These observations further confirm that the catalytically active V-species are different in the two cases. The slow build-up of the ring-hydroxylation products probably suggests that these are mainly produced over the framework V-species located inside the pores. Further confirmation of the presence of the V-species inside the pore system in sample B comes from an examination of the *o*/*p* ratio of the cresols in the product. Besides kinetic, mechanistic and structural factors (46), the *o*/*p* ratio of the product is also determined by the location of the active species in molecular sieve catalysts, with active centers inside the pore system producing more *p*-isomer than those outside (47). The smaller *o*/*p* ratio over sample B adds evidence to our earlier suggestion that the V-species is sample B are mostly located inside the pore system attached to the framework in defect sites. The V-species in sample A are probably located on the surface in

an easily extractable form; as a catalyst, sample A is similar to V-impregnated silicalite and pure NH_4VO_3.

A summary of the results of the various studies is presented below:

1. Analytical data indicate that the pick up of V^{4+} and V^{5+} by the crystalline phase is related to the concentration of the respective V-ions in the gel phase. However, while 84% of the V^{4+} ions in the acidic gel is picked up by the crystalline material, only 50% of the V^{5+} ions are picked up from the alkaline gel. More V-ions are extracted out by NH_4OAC solution (after calcination) from the sample from the acidic gel than from the alkaline gel.

2. XRD data indicate that the samples are highly crystalline. There is a phase transformation during the calcination of the sample A. The expansion of the unit cell volume is due to framework V-species present in the sample B.

3. Scanning electron micrographs reveal the formation of apparently defect-free large crystals when synthesized from the acidic medium. Alkaline synthesis leads to submicrometer particles.

4. TG-DTA studies reveal that the V-ions are in intimate contact with the template molecules only in the sample synthesized in an alkaline medium.

5. EPR experiments indicate that in the gel phase, V^{4+} species are present as freely mobile VO^{2+} ions (sample A) and in a distorted Oh environment (sample B). In the as-synthesized sample A, V^{4+} ions are in an agglomerated (polymeric) state, whereas, in sample B, they are well dispersed in an Oh environment. The polymeric V^{4+} species present in sample A are more difficult to oxidize or reduce than the framework V^{5+} species present in the sample B.

6. UV–visible spectra suggest that distorted Td–V^{5+} species are present in the as-synthesized and calcined forms of the sample B, while both the Td and Oh V-species are present in the calcined form of the sample A.

7. The IR band at 969 cm^{-1} attributed to Si–O^- linkages is related to the presence of nonextractable V^{5+} species.

8. NMR experiments indicate that monomeric HVO_4^{2-}, polymeric $V_2O_7^{4-}$, and the protonated species ($HV_2O_7^{3-}$) are present in the alkaline gel. Distorted Td–V^{5+} species are present in sample B whereas polymeric V-species with Td (like NH_4VO_3) and Oh (like V_2O_5) environment are present in the sample A. ^{29}Si MAS NMR indicate the absence of defect sites in sample A whereas defect sites are present in the sample B. The broadening of the ^{29}Si spectrum of sample B indicates the distribution of V with Si in the lattice. The ^1H MAS NMR experiment indicates the presence of V–OH linkages from nonframework vanadium in calcined sample A.

9. The sample synthesized from the alkaline medium is much more active than the one synthesized from acidic medium. During the reaction, the vanadium ions are more easily leached out from the latter sample than from the former.

CONCLUSIONS

The synthesis of V-MFI in an acidic medium using fluoride ions gives defect free orthorhombic crystals which transform into a monoclinic symmetry on calcination. Synthesis in an acidic medium is unfavorable for the incorporation of vanadium in the framework. The V-species present in the sample prepared in acidic medium are mostly nonframework polymeric species with Td and Oh environments. Synthesis in alkaline media favours the incorporation of vanadium in the framework of MFI molecular sieves. These framework V-species are in a distorted Td environment located at the defect sites. These V-species undergo redox cycles easily and are catalytically active. Besides, the V-ions are not leached into the reaction medium from the above sample in contrast to the sample prepared from an acid medium.

ACKNOWLEDGMENTS

S.S. thanks IFCPAR, New Delhi for funding the project. T.S. thanks UGC New Delhi for research fellowship. We thank Dr. P. Massiani, Univ. of Pierre et Marie Curie, Paris, for helpful discussions.

REFERENCES

1. Miyamoto, A., Medhanavyn, D., and Inui, T., *Appl. Catal.* **28**, 89 (1986); *in* "Proceedings, 9th International Congress on Catalysis, Calgary, 1988" (M. J. Phillips and M. Ternan, Eds.), Vol. 1, p. 437. Chem. Inst. of Canada, Ottawa, Ontario, 1988.
2. Zatorski, L. W., Centi, G., Nieto, J. L., Trifiro, F., Bellussi, G., and Fattore, V., *Stud. Surf. Sci. Catal. B* **49**, 1243 (1989).
3. Trifiro, F., and Jiru, P., *Catal. Today* **3**, 519 (1991).
4. Rigutto, M. S., and Van Bekkum, H., *Appl. Catal.* **68**, L1 (1991).
5. Prasad Rao, P. R. H., Ramaswamy, A. V., and Ratnasamy, P., *J. Catal.* **137**, 225 (1992).
6. Ramaswamy, A. V., Sivasanker, S., and Ratnasamy, P., *Microporous Materials* **2**, 451 (1994).
7. Reddy, K. R., Ramaswamy, A. V., and Ratnasamy, P., *J. Catal.* **143**, 275 (1993).
8. Reddy, K. M., Moudrakovski, I., and Sayari, A., *J. Chem. Soc. Chem. Commun.*, 1049 (1994).
9. Tuel, A., and Ben Tarrit, Y., *Zeolites* **14**, 18 (1994).
10. Reddy, K. M., Moudrakovski, I., and Sayari, A., *J. Chem. Soc. Chem. Commun.*, 1491 (1994).
11. Kornatowski, J., Wichterlova, B., Rozwadowski, M., and Baur, W. H., *Stud. Surf. Sci. Catal.* **84**, 117 (1994).
12. Sen, T., Chatterjee, M., and Sivasanker, S., *J. Chem. Soc. Chem. Commun.*, 207 (1995).
13. Sen, T., Ramaswamy, V., Rajmohonan, P. R., Ganapathy, S., and Sivasanker, S., *J. Phys. Chem.*, in press.
14. Whittington, B. I., and Anderson, J. R., *J. Phys. Chem.* **95**, 3306 (1991).
15. Guth, J. L., Kessler, H., and Wey, R., *Pure Appl. Chem.* **58**, 1389 (1986).
16. Chezeau, J. M., Delmotte, L., Guth, J. L., and Soulard, M., *Zeolites* **9**, 78 (1989).
17. Axon, S. A., and Klinowski, J., *Appl. Catal.* **56**, L9 (1989).
18. Centi, G., Perathoner, S., Trifiro, F., Aboukais, A., Aissi, C. F., and Guelton, M., *J. Phys. Chem.* **96**, 2617 (1992).
19. Moudrakovski, I., Sayari, A., Ratcliffe, C. I., Ripmeester, J. A., and Preston, K. F., *J. Phys. Chem.* **98**, 10895 (1994).
20. Kolthoff, I. M., *in* "Treatise on Analytical Chemistry," Part II, Vol. 8, p. 226. Interscience, New York/London 1963.

21. Chasteen, N. D., *Struct. Bonding* **53**, 112 (1983).
22. Hay, D. G., and Jaeger, H., *J. Chem. Soc. Chem. Commun.*, 1433 (1984).
23. Perego, G., Bellusi, G., Corno, C., Taramasso, M., Buonomo, F., and Esposito, A., *in* "Developments in Zeolite Science and Technology" (Y. Murakami *et al.*, Eds.), p. 129. Elseveir, Amsterdam, 1986.
24. Wu, E. L., Lawton, S. L., Olson, D. H., Rohrmann, A. C., Jr., and Kokotailo, G. T., *J. Phys. Chem.* **83**, 2777 (1979).
25. Fyfe, C. A., Kokotailo, G. T., Strobl, H., Gies, H., Kennedy, G. J., Pasztor, C. T., and Barlow, G. E., *Stud. Surf. Sci. Catal.* **46**, 827 (1989).
26. Busca, G., Centi, G., Marchetti, L., and Trifiro, F., *Langmuir* **2**, 568 (1986).
27. Cavani, F., Centi, G., Feresti, E., Trifiro, F., and Busca, G., *J. Chem. Soc. Faraday Trans. 1* **84**, 237 (1988).
28. Davidson, A., and Che, M., *J. Phys. Chem.* **96**, 9909 (1992).
29. Hush, N. S., and Hobba, R., *J. Prog. Inorg. Chem.* **10**, 259 (1968).
30. Selbin, J., *Chem. Rev.* **65**, 153 (1965).
31. So, H., and Pope, M. T., *Inorg. Chem.* **11**, 1441 (1972).
32. Iwamoto, M., Furukawa, H., Matsukami, K., Takenaka, T., and Kagawa, S., *J. Am. Chem. Soc.* **105**, 3719 (1983).
33. Ronde, H., and Snijders, J. G., *Chem. Phys. Lett.* **50**, 282 (1977).
34. Jhung, S. H., Uh, Y. S., and Chon, H., *Appl. Catal.* **62**, 61 (1990).
35. Taramasso, M., Perego, G., and Notari, B., U.S. Patent 4 410 501 (1983).
36. Reddy, J. S., and Kumar, R., *J. Catal.* **130**, 440 (1991).
37. Camblor, M. A., Corma, A., and Perez-pariente, J., *J. Chem. Soc., Chem. Commun.* 557 (1993).
38. Boccuti, M. R., Rao, K. M., Zecchina, A., Leofanti, G., and Petrini, G., *in* "Structure and Reactivity of Surfaces" (C. A. Morterra, A. Zecchina, and G. Costs, Eds.). Studies in Surface Science and Catalysis, Vol. 48, p. 133. Elsevier, Amsterdam, 1989.
39. Howarth, O. W., and Richards, R. E., *J. Chem. Soc.*, 864 (1965).
40. O'Donnell, S. E., and Pope, M. T., *J. Chem. Soc. Dalton Trans.*, 2290 (1976).
41. Lapina, O. B., Mastikhin, V. M., Shubin, A., Krasilnikov, V. N., and Zamaraev, K. I., *Prog. NMR Spectrosc.* **24**, 457 (1992).
42. Eckert, H., and Wachs, I. E., *J. Phys. Chem.* **93**, 6796 (1989).
43. Taouk, B., Guelton, M., Grimblot, J., and Bonnell, J. P., *J. Phys. Chem.* **92**, 6700 (1988).
44. Engelhardt, G., and Michel, D., "High Resolution Solid State NMR of Silicates and Zeolites," Wiley, New York, 1987.
45. Hauka, S., Lakomaa, E. L., and Root, A., *J. Phys. Chem.* **97**, 5085 (1993).
46. Ingold, C. K., "Structure and Mechanism in Organic Chemistry," 2nd ed. Bell and Hyman, London, 1967.
47. Tuel, A., Moussa-Khouzami, S., Ben Taarit, Y., and Naccache, C., *J. Mol. Catal.* **68**, 45 (1991).